Int. J. Bio-Inorg. Hybd. Nanomat., Vol. 1, No. 2 (2012), 115-122

International Journal of Bio-Inorganic Hybrid Nanomaterial

Photocatalytic and Magnetic Behavior of Fe_2TiO_5-5A Zeolite Nanocomposites

Elnaz Khosravi[1], Maryam Kargar Razi[1], Morteza Enhessari[2*]

[1] *Department of Chemistry, North Tehran Branch, Islamic Azad University, Tehran, P.O. Box: 19136, Iran*

[2] *Department of Chemistry, Naragh Branch, Islamic Azad University,Naragh, P.O. Box: 37961-58719, Iran*

Received: 18 March 2012; Accepted: 26 May 2012

ABSTRACT

In this paper we report synthesis of Fe_2TiO_5-5A zeolite (Z5A) nanocomposites with 5%, 10% and 20% weight percent of Fe_2TiO_5 in 5A zeolite in stearic acid media after calcination of the gel samples obtained at 600-900°C for 2 hrs. The powder X-RAY diffraction (XRD) patterns have been used for characterization of the prepared samples. The Scanning Electron Microscopy (SEM) images and X-ray Energy Dispersion (EDX) results were used to determine the size and composition of Fe_2TiO_5-Z5A nanocomposites. Differential porosity value of Fe_2TiO_5-Z5A nanocomposite samples in comparison with the 5A zeolite were obtained by Brunauer-Emmett-Teller (BET) method. A Vibrating Sample Magnetometer (VSM) was used to determine magnetic behavior of 20% Fe_2TiO_5-Z5A and pure Fe_2TiO_5. The results indicated the change of Ferromagnetism to the superparamagnetism behavior due to the small particle size and a high value of calcan and methylene blue degradation (63 and 99% respectively) for 20% Fe_2TiO_5-Z5A.

Keyword: Fe_2TiO_5 -5A zeolite; Superparamagnetism; Sol-gel method; Photocatalytic activity; Magnetic properties.

1. INTRODUCTION

In recent years interest has been focused on the use of semiconductor nanomaterials as photocatalysts for removal of the organic and inorganic species from aqueous or gas phase environment. These kind of materials have been suggested in the environmental protection due to their ability in oxidizing organic and inorganic substances [1, 2]. On the other hand, Zeolites with a high surface area, unique nanoscaled porous structure and ion exchange properties offer a new opportunity for their utilization as a matrix in the design of efficient photocatalytic systems [3]. Among them, aluminosili-

(*) Corresponding Author - e-mail: Enhessari@iau-naragh.ac.ir

cate zeolites showed considerable promise in the promotion of stabilization and photochemically generated redox species as well [4]. The 5A zeolite that represented by the formula $Na_{12}[(AlO_2)_{12}(SiO_2)_{12}]$. $27H_2O$ [5] possessing effective channel diameter of uniform size [3] is a good example. Titanium substituted iron oxides are widespread in nature and represent an important mineral resource for the commercial obtainment of both iron and titanium compounds [5]. Pseudobrookite, a natural mineral, is present in igneous and metamorphic rocks and has magnetic properties [6-7]. Fe_2TiO_5 can be used as material for optical filters and for photocatalytic applications [8].

The combination of different material allows for the creation of a completely new composite material with a wide range of functional properties: mechanical, chemical, electrical, magnetic, and optical and many others [9-14]. The nanocomposite is prepared by a various techniques such as hydrothermal precipitation [15], sol-gel methods [16], vapor deposition [17] and RF sputtering [18].

One typical wet chemistry synthesis method,stearic acid gel, because of the good chemical process control [19-21] was applied to synthesize titanium based oxide containing metals such as manganese titanate [20], cobalt titanate [21], iron titanate [22], bismuth titanate [23], nickel titanate [24], cadmium titanate [25], barium titanate [26] with wide applications.

Previous works have mainly emphasized on the synthetic zeolites such as ZSM-5 [27], A-zeolite [27], HZSM-5 [28-30], MCM-41 [30], X-zeolites [31], Y-zeolite [31,32], HY-zeolites [29,30], Hb-zeolites [29], Hβ-zeolite [30], β-zeolite [33], USY-zeolite[34], MOR-zeolite[35], Natural zeolite (clinoptilolite) [2] etc., as the substrates of TiO_2. Recently, Enhessari and et al. have synthesized and investigated photocatalytic properties of $MnTiO_3$-Zeolite-Y nanocomposites [36].

In this study, Fe_2TiO_5-Z5A nanocomposites were synthesized via stearic acid gel method. In addition, characterization, magnetic and photocatalytic properties of the nanocomposites were investigated.

2. EXPERIMENTAL

2.1. Materials

The chemicals used in this study were titanium (IV) n-butoxide, as a titanium source purchased from Aldrich chemical, iron acethyleacetonate as iron source and stearic acid as a complexing reagent from Merck and 5A Zeolite which was purchased from SPAG Co.

2.2. Preparation of Fe_2TiO_5 nanopowder

Fe_2TiO_5 powders was prepared by sol-gel method using iron acetyl acetonate, tetra-n-butyl titanate and stearic acid as described in [37]. Dried gel obtained was then calcined at 900°C for 2 h.

2.3. Preparation of Fe_2TiO_5-Z5A (5-10-20) % nanocomposites

The Fe_2TiO_5-Z5A in 5-10 and 20 at % nanocomposites were prepared by sol-gel method. In this procedure, iron acethyle acetonate was added to the melted stearic acid and dissolved to form a dark red-brown transparent solution. Then titanium (IV) n-butoxide was slowly dropped into the above solution. Further stoichiometric amounts of 5A zeolite introduced to the mixed solution and stirred completely to obtain the sol, then the gel. The gels were dried in oven at 100°C for 12 h and calcined at 600-700-800-900°C to obtain Fe_2TiO_5-Z5A nanocomposites.

2.4. Characterization

To investigate the phase composition and crystalline size distribution of the nanocomposites after calcinations, x-ray diffraction (XRD) measurements were performed. XRD was recorded of Philips x-pert diffractometer in the 2θ range of 5-90° using Cu Kα radiation. The chemical identity of the products was determined by comparing the experimental x-ray patterns to standard complied by the Joint Committee on powder diffraction and standards (JCPDS). The morphology of the product was studied by scanning electron microscopy (SEM, Philips XL30). Semiquantative analysis were carried out on an energy-dispersive x-ray spectrometer (EDAX) connected to XL30

Philips scanning electron microscope. The UV-Vis absorption spectra were obtain with 4802 Unico spectrophotometer in the region of 200-800 nm. To compare surface areas, total pore volume and average pore diameter, BET analysis was studied by BelSorp Mini BEL Co. equipment. To investigate magnetic properties MDK6 equipment was used.

3. RESULTS AND DISCUSSION

3.1. XRD patterns

Figure 1 shows the XRD patterns of 20% Fe_2TiO_5 -Z5A nanocomposites after heat treatment from 600°C to 900°C for 2 hours in temperature programmable furnace. This Figure 1a shows the

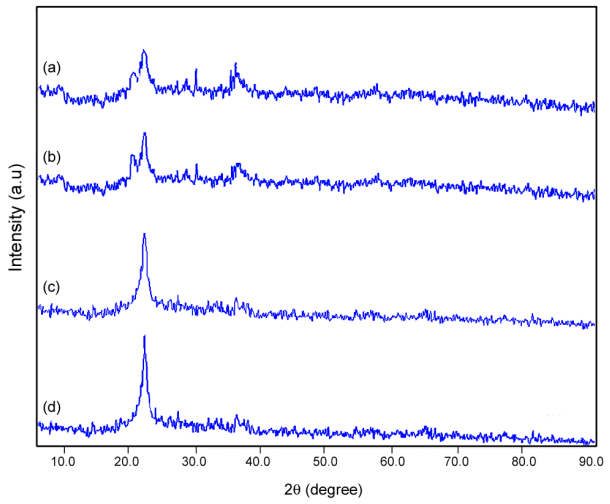

Figure 1: *XRD patterns of: 20% Fe_2TiO_5-Z5A (20%) nanocomposites calcined at: a) 600°; b) 700°; c) 800°; d) and 900°.*

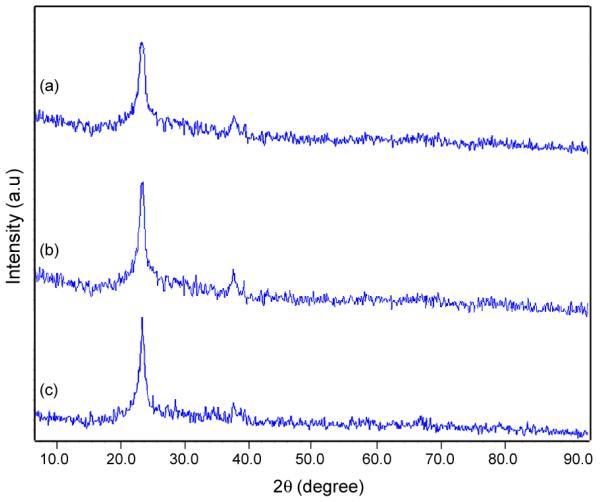

Figure 2: *XRD patterns of 5% (a) -10% (b) -20% (c) Fe_2TiO_5-Z5A nanocomposites calcined at 900°.*

characteristic peaks appeared at 2θ = 27.39°, 19.323°, 35.416° which are those of TiO_2, Fe_2O_3 and 5A zeolite. Figure 1b shows the characteristic peaks appeared at 2θ = 19.323°, 35.416° and confirms the presence of Fe_2TiO_5 and 5A zeolite phase calcined at 700°C. Further in Figures 1c and 1d by increasing the calcination temperatures up to 800°C and 900°C, the 5A zeolite phase decreased by increasing Fe_2TiO_5 phase. Figure 2 compares XRD patterns of the (5-10-20) % Fe_2TiO_5-Z5A nanocomposites calcined at 900°C for 2 h. This XRD patterns show clearly that the intensity of Fe_2TiO_5 typical peak in the 20% nanocomposite is higher. The size of the prepared nanocomposites with (5-10-20) % Fe_2TiO_5 nanoparticles determined using Sherrer formula were in the range of 48-70 nm.

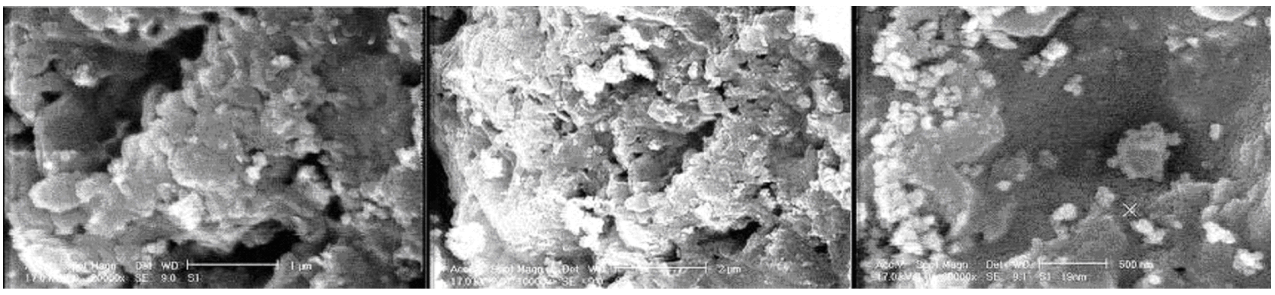

(a) (b) (c)

Figure 3: *SEM images of 5% (a) - 10% (b) - 20% (c) Fe_2TiO_5-Z5A nanocomposites.*

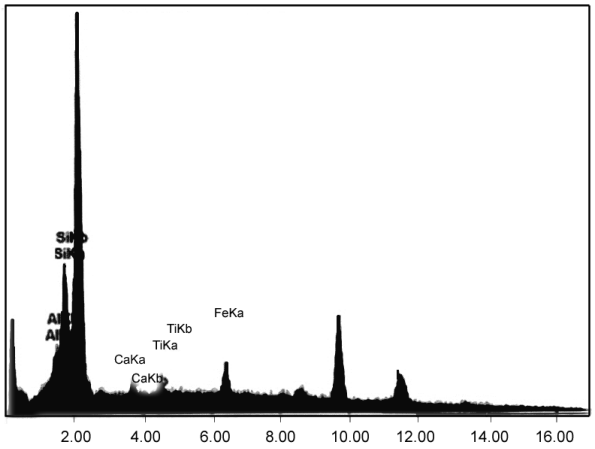

Figure 4: *EDX analysis data of Fe_2TiO_5-Z5A nanocomposite (20%).*

3.2. SEM and EDX studies

Figure 3a,b,c shows the typical SEM of (5-10-20)% nanocomposites respectively. The stoichiometry of the obtained 20% nanocomposite was demonstrated by EDX measurement in Figure 4.

3.3. VSM result

Figure 5 shows vibrating sample magnetism curves of Fe_2TiO_5 nanopowders and 20% Fe_2TiO_5 Z-5A nanocomposites calcined at 900°C. This curve clearly show that the ferromagnetic behavior of

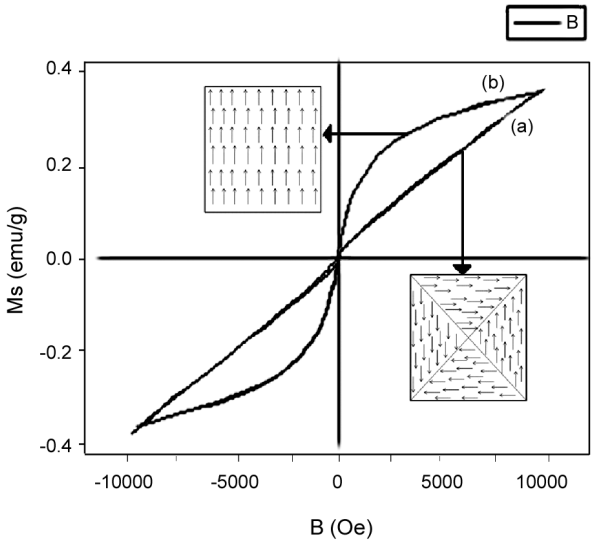

Figure 5: *VSM curves of: a) Fe_2TiO_5 nanocomposite powders[37]; b) 20% Fe_2TiO_5 -Z 5A nanocomposite calcined at 900°C.*

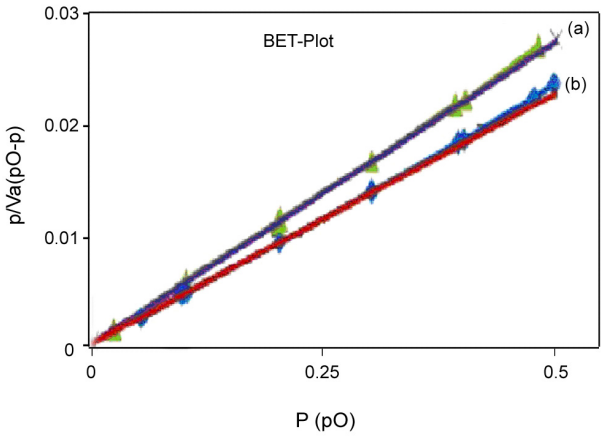

Figure 6: *BET comparison of 20% Fe_2TiO_5-5A Zeolite nanocomposite (a) and Z-5A (b).*

Fe_2TiO_5 nanopowders with a room temperature remnant magnetization (Mr = ~0.02 emu/g) and very low coercivity (Hc) has been changed to a superparamanetic one with Mr = 0 and coercivity, Hc = 0 Oe in 20% Fe_2TiO_5 Z- 5A nanocomposite. This change of magnetic property can be expected more prominently for smaller particles size in a larger surface-to-volume ratio.

3.4. BET comparison

Figure 6 compares the BET (Brunauer-Emmett-Teller) analysis 20% Fe_2TiO_5 -Z 5A (a) and of Z 5A zeolite (b). The results are presented in table 1. The difference among the specific surface and the average pore diameter of Z-5A and the nanocomposite shows that the growth of nanoparticles acts as a dam against the closure of the spaces in the structure of Z- 5A. This is responsible for increment of the average diameter of pores. It also shows that the nanoparticles are distributed into the zeolite. This combined with increment of average pore diameter and decrement of specific surface of zeolite. It is noteworthy that the small volume of pores can also confirms the presence of nanoparticles on the zeolite cavities [35].

3.5. UV-Vis spectra

3.5.1 UV-Vis spectra of methylene blue

Figure 7 shows the UV-Vis spectra of methylene blue degradation (20 ppm solution) by (5-10-20) %

Table 1: *BET comparison results.*

	Z-5A Zeolite	nanocomposite	Unit
Vm	22.07	18.348	[$cm^3.g^{-1}$]
$a_{s,BET}$	96.075	79.86	[$m2.g^{-1}$]
C	119.81	119.81	Cte
Total pore volume	0.2547	0.237	[$cm^3.g^{-1}$]
Average pore diameter	10.605	11.87	[nm]

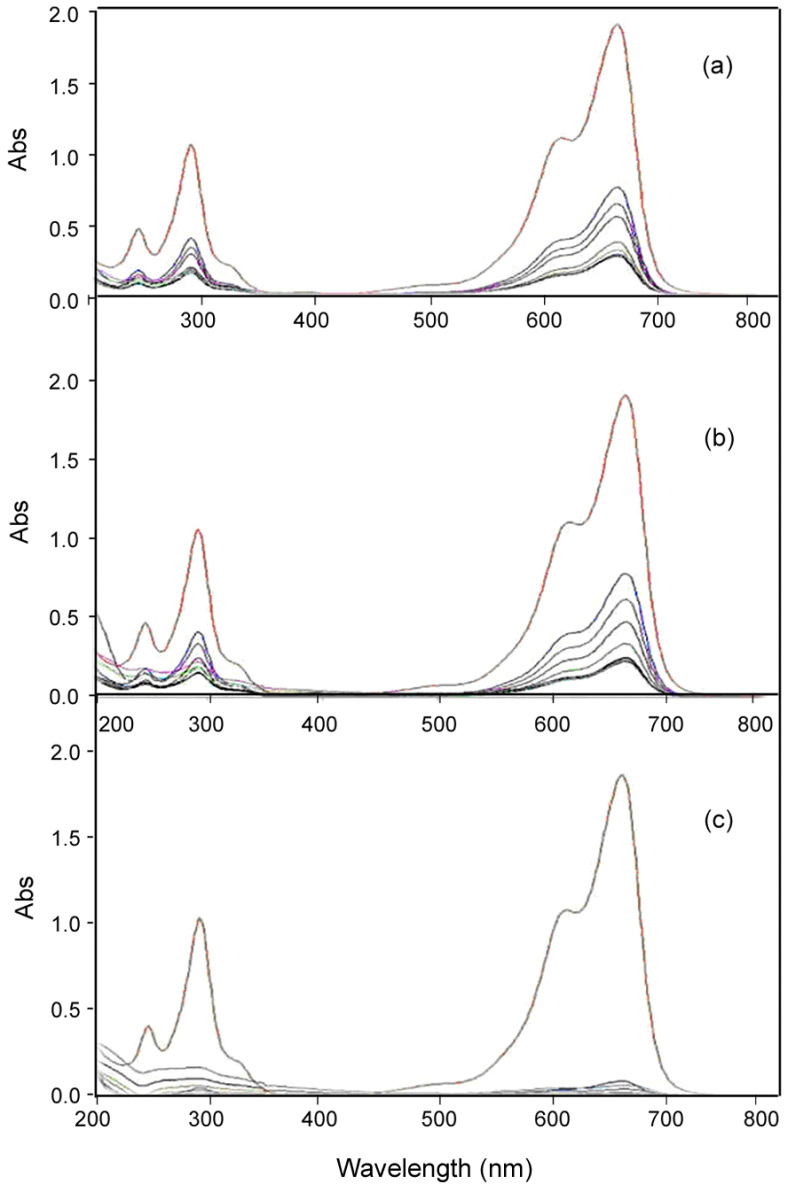

Figure 7: *UV-Vis spectra of 5% (a) -10% (b) -20% (c) Fe_2TiO_5 -Z5A nanocomposites.*

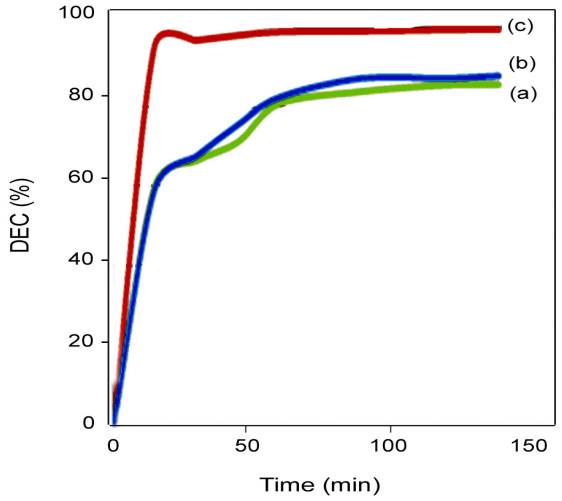

Figure 8: *Methylene blue degradation of 5% (a) -10% (b) -20% (c) Fe_2TiO_5-Z5A nanocomposites for decolorization.*

Fe_2TiO_5-5A zeolite nanocomposites in the wavelength range of 200-800 nm. It proves that the 20% nanocomposite is more effective to decompose the structure of methylene blue molecules. It was concluded from figure 7 that the 20% nanocomposite can decolorize the 20 ppm solution of methylene blue up to 99% in 60 min.

3.5.2 UV-Vis spectra of calcon

Figure 9 shows the UV-Vis spectra that confirms the degradation of calcon 20 ppm solution by (5-10-20)% Fe_2TiO_5-Z 5A nanocomposite in the wavelength range of 200-800 nm. It proves that the 20% nanocomposite is more effective to decompose the structure of calcon molecules. It was concluded from Figure 10 that the 20% nanocomposite can decolorize the 20 ppm solution of calcon

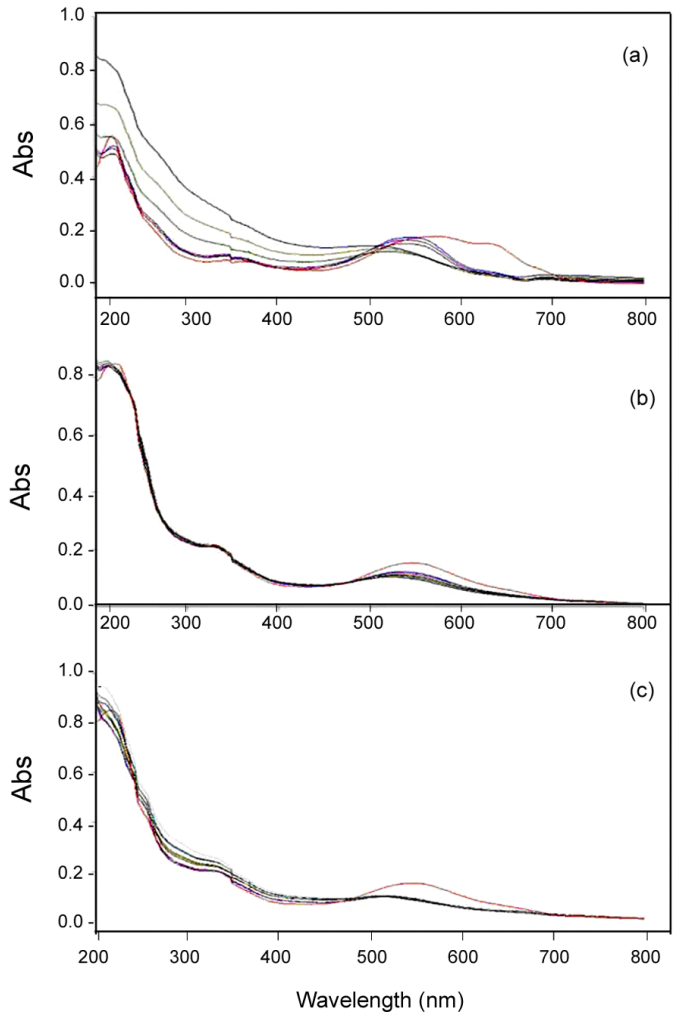

Figure 9: *UV-Vis spectra of 5% (a) -10% (b) -20% (c) Fe_2TiO_5 -5A zeolite nanocomposites.*

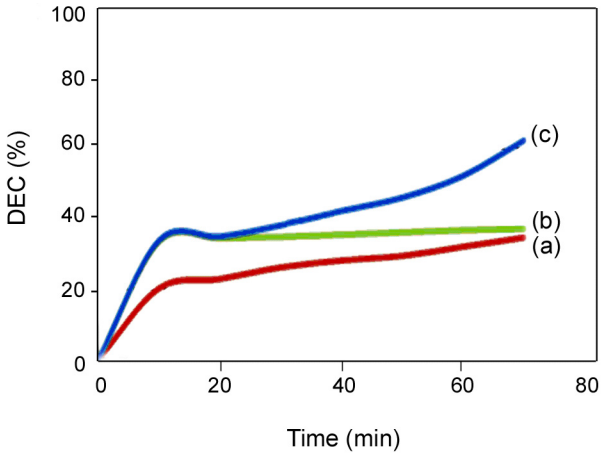

Figure 10: *Degradation comparison of 5% (a) -10% (b) -20% (c) Fe_2TiO_5-Z 5A nanocomposites for calcon decolorization.*

up to 63% in 60 min.

4. CONCLUSIONS

Fe_2TiO_5-Z 5A nanocomposites were synthesized with (5-10-20 w%) by sol-gel method. The gel was calcinated at 600-700-800-900°C for 2 hours. The presence of rhombohedral phase of Fe_2TiO_5 in 5A zeolite matrix was confirmed by XRD. Scaning electron microscopy showed that the particale sizes are between 19-29 nm. X-ray diffraction patterns and BET analysis showed the presence and growth of Fe_2TiO_5 nanoparticles in 5A zeolite. The VSM results showed the superparamagnetic properties of 20% nanocomposite. The photocatalytic activity of nanocomposites was evaluated by degradation of methylene blue and calcon reagents in aqueous solution. It was concluded from UV-Vis spectra that the 20% nanocomposite can decolorize the 20 ppm solution of methylene blue up to 99% in 60 min and decolorize the 20 ppm solution of calcon up to 63% in 60 min. The best results belongs to 20% Fe_2TiO_5-Z5A nanocomposite.

REFERENCES

1. Fox M.A., Dulay M.T., *Chem. Rev.*, **93**(1993), 341.
2. Wang C., Shi H., Li Y., *App. Surf. Sci.*, **257**(2011), 6873.
3. D.W. Breck, 1974. Zeolite Molecular Sieves, Structure Chemistry and Use, John Wiley and Sons, New York.
4. Dutta P.K., Tureville W., *J. Phys. Chem.*, **96**(1992), 23.
5. Ruthven D.M., Derrah R.I., *J. Chem. Soc.*, Faraday Trans. 1, **68**(1972), 2332.
6. Guo W.Q., Malus S., Ryan D.H., Altounian Z., J. Phys., *Condens. Matter*, **11**(1999), 6337.
7. S.M. Swiata, 1985. Wydawnictwo Geologiczne-Warszawa., Perkas N., Koltypin Y., Palchik O., Gedanken A., Chandrasekaran S., *Appl. Catal. A*, **209**(2001), 125.
8. Kundo T.K., Chakaravorty D., *Appl. Phys. Lett.*, **66**(1995), 3576.
9. Wang J.P., Han D.H., Luo H.L., Gao N.F., Liu Y.Y., *Magn. Mater*, **135**(1994), 251.
10. D. Ozimina, Kielce, 2006. in Polish.
11. I. Gruin, P.W.N. Warsaw, 2003. in Polish.
12. A. Boczkowska, J. Kapuciski, Z. Leidemann, D. Witemberg-Perzyk, S. Wojciechowski, 2003. in Polish.
13. L.A. Dobrzaki, W.N.T. Warsaw, 2006. in Polish.
14. Shang Y., Weert G.V., *Hidrometallurgy*, **33**(1993), 273.
15. Roy R.A., Roy R., *Matter Res Bull*, **19**(1984), 169.
16. Wang J.P., Luo H.L., *Magn. Mater*, **131**(1994), 54.
17. Abeles B., Sheng P., Coutts M.D., Arie Y., *Adv. Phys.*, **15**(1976), 2328.
18. Phani A.R., Ruggieri F., passa cantando M., *S. Ceramics International*, **34**(2008), 205.
19. Haraguchi K., *Curr. Opine. Solid st. Mater. Sci.*, **11**(2007), 47.
20. Shen G.X., Chen Y.C., Lin C.J., *J. Thin solid Films*, **489**(2005), 130.
21. Enhessari M., Parviz A., Ozaee K. and Karamali E., *J. Exp. Nanosci.*, **5**(2010), 61.
22. Khaleel A., Sol-gel synthesis, colloids and surfaces. *A: phsicochem .eng. aspects*, **346**(2009), 130.
23. Madeswaran S., Giridharan N.V., Jayavel R.,

Mater. Chem. Phys., **80**(2003), 23.
24. Sadjadi M.S., Zare K., Khanahmadzadeh S., Enhessari M., *Mater. Let*, **62**(2008), 3679.
25. Wang H., Zhang X., Huang A., Xu M., Zhu H., Wang B., Yan H., Yoshikura M.A., *J. Cryst. Growth*, **246**(2002), 150.
26. Xu H., Gao L., *Mater. Let*, **57**(2002), 490.
27. Xu Y.M., Langford C.H., *J. Phys. Chem*., **99**(1995), 11501.
28. Durgakumari V., Subrahmanyam M., Subba Rao K.V., Ratnamala A., Noor-jahan M., Tanaka K., *Appl. Catal. A*, **234**(2002), 155.
29. Shankar M.V., Anandan S., Venkatachalam N., Arabindoo B., Murugesan V., *Chemosphere*, **63**(2006), 1014.
30. Mahalakshmi M., Vishnu Priya S., Banumathi Arabindoo M., Palanichamy V., Murugesan J., *J. Hazard. Mater*, **161**(2009), 336.
31. Xu Y.M., Langford C.H., *J. Phys. Chem*., **101**(B) (1997), 3115.
32. Alvaro M., Carbonell E., Fornes V., García H., *Chem. Phys. Chem*., (2006), 200.
33. Yamashita H., Kawasaki S., Yuan S., Maekawa K., Anpo M., Matsumura M., *Catal. Today*, **126**(2007), 375.
34. Aramendía M.A., Colmenares J.C., López-Fernández S., Marinas A., Mari-nas J.M., Urbano F.J., *Catal. Today*, **129**(2007), 102.
35. Takeuchi M., Deguchi J., Hidaka M., Sakai S., Woo K., Choi P.P., Park J.K., Anpo M., *Appl. Catal. B*, **89**(2009), 406.
36. Enhessari M., Kargar-Razi M., Moarefi P., Parviz A., *JNS*, **2**(2012), 119-125.
37. Enhessari M., Kargar Razi M., Etemad L., Parviz A., Sakhaei M., *J. exp. Nanosci*, (2012), DOI:10.1080/17458080.2011.649432.